Chemical Physics 28 (1978) 319–329

ROTATIONAL INELASTICITY IN HIGH-ENERGY H_2–H_2 COLLISIONS *

Ramakrishna RAMASWAMY, Herschel RABITZ ‡
Department of Chemistry, Princeton University, Princeton, New Jersey 08540, USA

and

Sheldon GREEN
NASA Institute for Space Studies, Goddard Space Flight Center, New York, New York 10025, USA and Department of Chemistry, Columbia University, New York, New York 10027, USA

Received 11 October 1977

Rotational cross sections for transitions in the H_2–H_2 system have been calculated for energies up to ≈ 2.0 eV and for rotor levels up to $j = 11$ in the effective potential approximation. The cases of para H_2–para H_2, ortho H_2–ortho H_2 and ortho H_2–para H_2 are considered. Correlations and trends in the cross sections have been examined, and it is shown that the high-energy collisions are dominated by coupling effects. The results of this analysis also suggest that the collision process may be profitably viewed as a diffusion of probability among the levels.

1. Introduction

Since the rotational energy spacing for most molecules is small compared with thermal energies, rotational relaxation typically involves many quantum levels. Experimental measurements of relaxation times, therefore, give only some average of the many *state-to-state* rates which contribute to the overall process [1]. Attemps to obtain information about individual rates from such measurements require some prior assumptions about the relative values of different rates. This can be misleading since non-unique sets of rates can give the same average relaxation time, so the assumptions tend to be self-fulfilling. Alternatively, measurements can be made at low temperatures where only one rate (between the ground and first excited state) is important; of course this provides information about only this one *state-to-state* rate. For these reasons relatively little has been learned about the relative rates of different transitions in relaxation processes. It has not generally been known which rates dominate a specific experimental situation.

For some simple systems this problem has been remedied somewhat with the availability of accurate quantum calculations. The theoretical approach automatically gives detailed information about *state-to-state* processes. By taking appropriate averages of this detailed information, it is possible to predict relaxation times, and generally very good agreement with experimental values has been obtained for the systems where this has now been done. More importantly, these studies are beginning to provide insight into the nature of energy transfer in typical molecular collisions. Simple but accurate models and rules of thumb are beginning to emerge.

Most of the calculations to date have considered excitation of linear rigid rotors by collision with atoms. A few studies have also considered vibration–rotation excitation of diatomics hit by atoms and rotational excitation of polyatomic molecules by atoms. Because of additional computational complications and expense, few studies of molecule–molecule collisions have been performed [2–4]. We have previously studied in some detail one of the simplest molecule–molecule systems: collisions of two H_2 molecules [5]. These earlier studies considered only the lowest few

* Research supported in part by ERDA and in part by NASA, Grant # NSG 7105.
‡ Alfred P. Sloan Fellow, Camille and Henry Dreyfus Teacher-Scholar.

rotational levels and relatively low collision energies. Because of astrophysical interest in these molecular rates, we have now extended these calculations to include twelve levels and collision energies up to a few electron volts (about 20000 K). Such a calculation produces several hundred state-to-state cross sections as a function of collision energy. In the present paper we attempt to extract the underlying trends from this body of data.

2. Background details of the calculation

The large number of "open" molecular levels at high collisional energies requires the solution of a large set of coupled equations. Even with this difficulty the problem is quite manageable with the use of appropriate effective hamiltonian methods [6]. Within this framework we have chosen to solve the scattering equations in the effective potential (EP) approximation; the pertinent scattering equations in this formalism have been presented earlier [2,3,6] and will not be repeated here. A number of semi-empirical and ab initio potentials have been calculated for the H_2–H_2 system. A comparison of the accuracy of some of these surfaces indicated that the ab initio surface of Merrifield and Ostlund [7] was the most satisfactory in describing the H_2–H_2 collisional system. This potential is employed in the present work ‡. The scattering calculations here treat the H_2 molecule as a rigid rotor. To gauge the effect of the vibrational "motion", the augmented surface of Ostlund [8] that does contain vibrational coordinate dependence was averaged over the ground state

$$V(R,\theta_1,\theta_2,\varphi_1-\varphi_2) = \langle 00|V(R,r_1,r_2,\theta_1,\theta_2,\varphi_1-\varphi_2)|00\rangle . \quad (1)$$

The vibrational coordinates of the two molecules are r_1 and r_2; the angular variables are denoted θ_1, θ_2 and $\varphi_1-\varphi_2$ [see fig. 1 of ref. [5] for the coordinate system used]. The wavefunction $\langle r_1 r_2|00\rangle$ is defined as

$$\langle r_1 r_2|00\rangle = \varphi_0(r_1)\,\varphi_0(r_2),$$

where $\varphi_0(r)$ is a ground state Morse-oscillator wavefunction. The separability of the vibration–rotation wavefunction as a product of the vibrational wavefunction and spherical harmonics has been assumed. This approximation is convenient but can be dropped if necessary. Cross sections obtained by using the averaged potential of eq. (1) are only slightly (< 5%) larger than those from the rigid-rotor potential [7].

Vibrational transitions are indeed possible at energies greater than $\simeq 0.5$ eV ‡, but the magnitude of vibrationally inelastic cross sections is much smaller than the dominant rotational cross sections [10]. Although the precise value of some rotational cross sections could depend on the presence of open or closed vibrational states, the essential features of the rotational structure are probably not affected. From the computational point of view, inclusion of vibrational states in the basis set would have drastically increased the complexity of the problem. This study is therefore restricted to pure rotational transitions in oH$_2$–oH$_2$, pH$_2$–pH$_2$ and oH$_2$–pH$_2$ collisions.

The energy dependence of the principal cross sections (i.e., those $> 10^{-5}$ Å^2) was fit to a quadratic form in the initial kinetic energy, $\mathcal{E}$

$$\sigma_{i\to j}(E_{\rm tot} = \mathcal{E}_i + \mathcal{E}) = a_{ij} + b_{ij}\mathcal{E} + c_{ij}\mathcal{E}^2 , \quad (2)$$

where $\mathcal{E}_i$ is the rotational energy of the initial state. The coefficients a, b and c are fitting parameters without any physical significance. The range of validity of these fits and the tables of the coefficients have been published elsewhere [11].

The basis sets used in these EP calculations are shown in fig. 1. Limited basis set exact close coupled (CC) and coupled states (CS) [6] effective hamiltonian calculations were also made in the case of oH$_2$–pH$_2$ collisions. These serve as a guide for judging the accuracy of the EP results. The general behavior of the H_2–H_2 system is examined in the following sections of this paper. The overall trends are discussed and various correlations are made to draw together the large amount of information generated in these calculations.

‡ Some parallel calculations were made using the Gallup CI potential [9]. The Ostlund and Gallup potentials do not differ significantly in the region under study here, and the overall results do not differ much either.

‡ All energies are measured from the ground rotation–vibration state, $n_1 j_1 n_2 j_2 = 0000$.

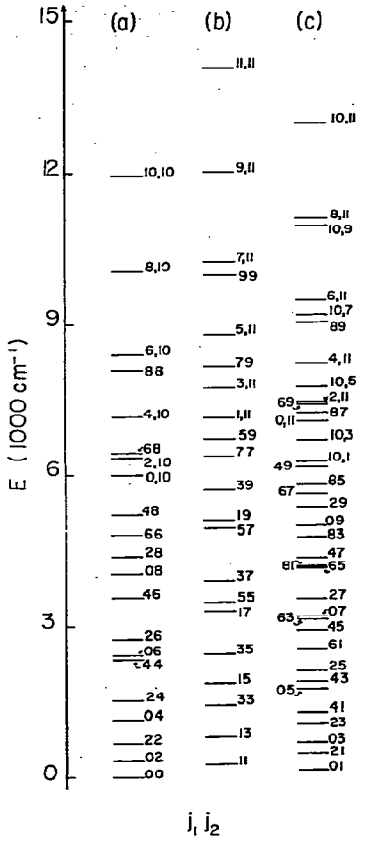

Fig. 1. Energy spacing for the three systems studied. (a) Para H_2–para H_2; (b) ortho H_2–ortho H_2; (c) para H_2–ortho H_2.

3. Results

3.1. General features of the cross sections

In identical molecule collisions the total cross section is a sum of direct (d) and exchange (e) terms

$$\sigma^{\mathrm{tot}}(j_1 j_2 \to j_1' j_2'; E) = \sigma^{(\mathrm{d})}(j_1 j_2 \to j_1' j_2'; E) + \sigma^{(\mathrm{e})}(j_1 j_2 \to j_2' j_1'; E). \quad (3)$$

Obtaining either of these contributions separately involves approximately twice the expense of obtaining σ^{tot} alone; all cross sections reported here are σ^{tot}. In oH_2–pH_2 collisions the exchange term is identically zero since we are not considering reactive collisions. The cross sections in this case consist of just the direct term and are therefore easier to interpret. Fig. 2 shows the total cross sections at a fixed total energy for all possible transitions within the basis shown in fig. 1c. The states are ordered energetically so that the upper right triangle depicts excitations and the lower part, deexcitation. The *fixed* total energy effects larger cross sections (i.e., darker regions) in the upper left corner of the diagram. It may also be seen that along a row or column (i.e., for a fixed initial or final state), the magnitude of the cross section does not necessarily fall off in a monotonic fashion from the diagonal. This indicates the importance of coupling factors over energetics. Lack of "reflection symmetry" with respect to the diagonal is mainly due to m-state statistical factors. The prominent feature emerging from the general structure of this diagram is that for any particular initial state there are relatively few final states for which transitions are of significant magnitude.

Figs. 3a and 3b dramatize the importance of coupling in these transitions. Cross sections from particular initial states to all possible final states are shown at a fixed total energy. Each curve [†] of cross sections $\sigma(j_1 j_2 \to j_1' j_2'; E)$ is labeled by the initial state $j_1 j_2$. Fig. 3a includes the initial states $j_1 1, j_1 = 0, 2, \ldots, 10$ and fig. 3b the states $0 j_2, j_2 = 1, 3, \ldots, 11$. The total energy, E_{tot}, in both cases is 16000 cm^{-1}. The diagrams share the prominent oscillatory behavior, wherein the cross section curves vary in a regular fashion over many orders of magnitude regardless of the initial state. The differences in the initial *kinetic* energies for the various curves contribute to the spread of the envelopes of each set of initial states. The oscillations in the two figures are out of phase in the sense that the local minima of fig. 3a correspond to final states yielding local maxima in fig. 3b and vice versa.

The generally rather complicated behavior in these figures can be understood if we choose a parameter based on angular momentum differences rather than energy differences. An appropriate parameter that is more discriminating [‡] than the absolute change in an-

[†] The word "curve" here denotes the line segments connecting the consecutive points $\sigma(j_1 j_2 \to j_1' j_2'; E)$.

[‡] The appropriateness of this parameter can be seen by comparing the transitions $23 \to 69$ and $01 \to 011$, for example. While both transitions have $\Delta j = 10$, the R^2 values are 52 and 100, respectively. It may be added that R^2 is just one of many possible such parameters generally defined by $R^n = |j_1 - j_1'|^n + |j_2 - j_2'|^n, n \neq 0, 1$.

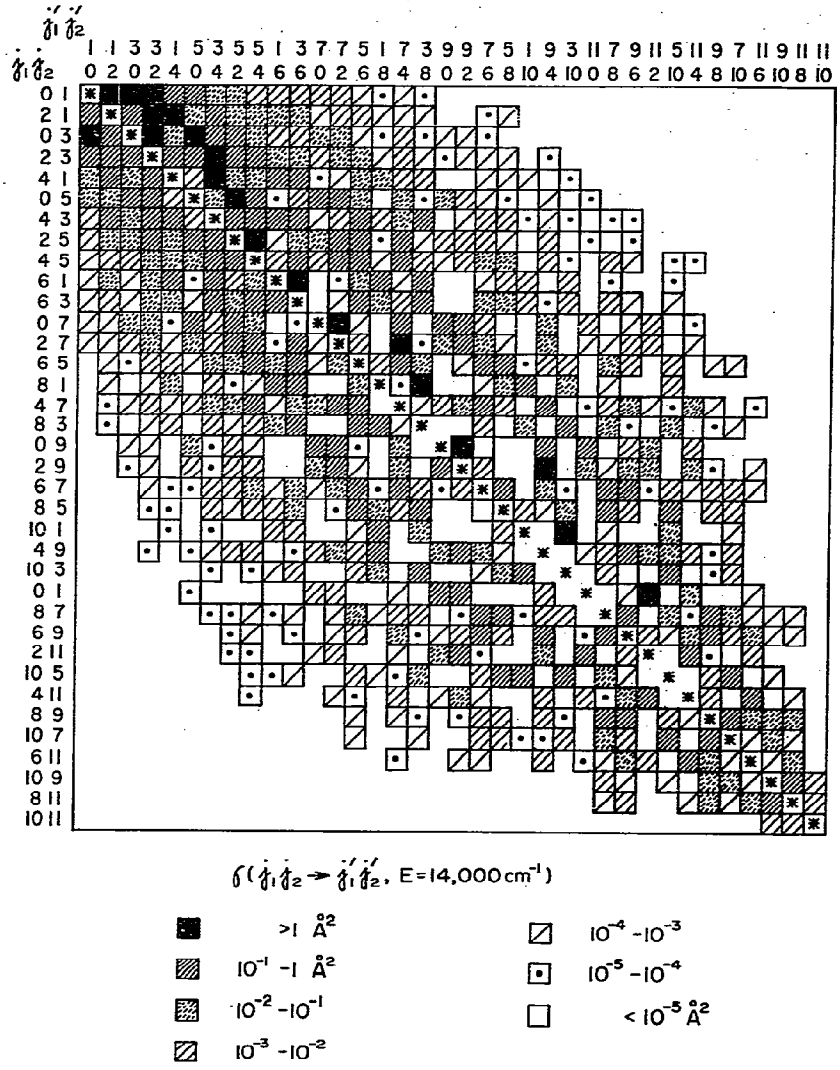

Fig. 2. Cross sections from all initial states to all final states in the basis of fig. 1c in oH_2–pH_2 collisions. The total energy is fixed at 14000 cm^{-1}.

gular momentum

$$\Delta j = |j_1 - j_1'| + |j_2 - j_2'|, \tag{3}$$

is R^2, defined as

$$R^2 = |j_1 - j_1'|^2 + |j_2 - j_2'|^2. \tag{4}$$

In fig. 3c the cross sections shown in figs. 3a and 3b are plotted as a function of R^2, again keeping the total energy fixed at 1600 cm^{-1}. While it can be seen that the cross sections are a function of this parameter, there is, however, a spread in the cross sections for each value of R^2. Since this spread probably arises from both energetic and other coupling effects, it is not possible to precisely parameterize the cross sections in terms of R^2.

Now consider the $\sigma(01 \to j_1' j_2'; E)$ curve in figs. 3a and 3b, which seems to differ in behavior from the other curves. The state 01 has both molecules in the

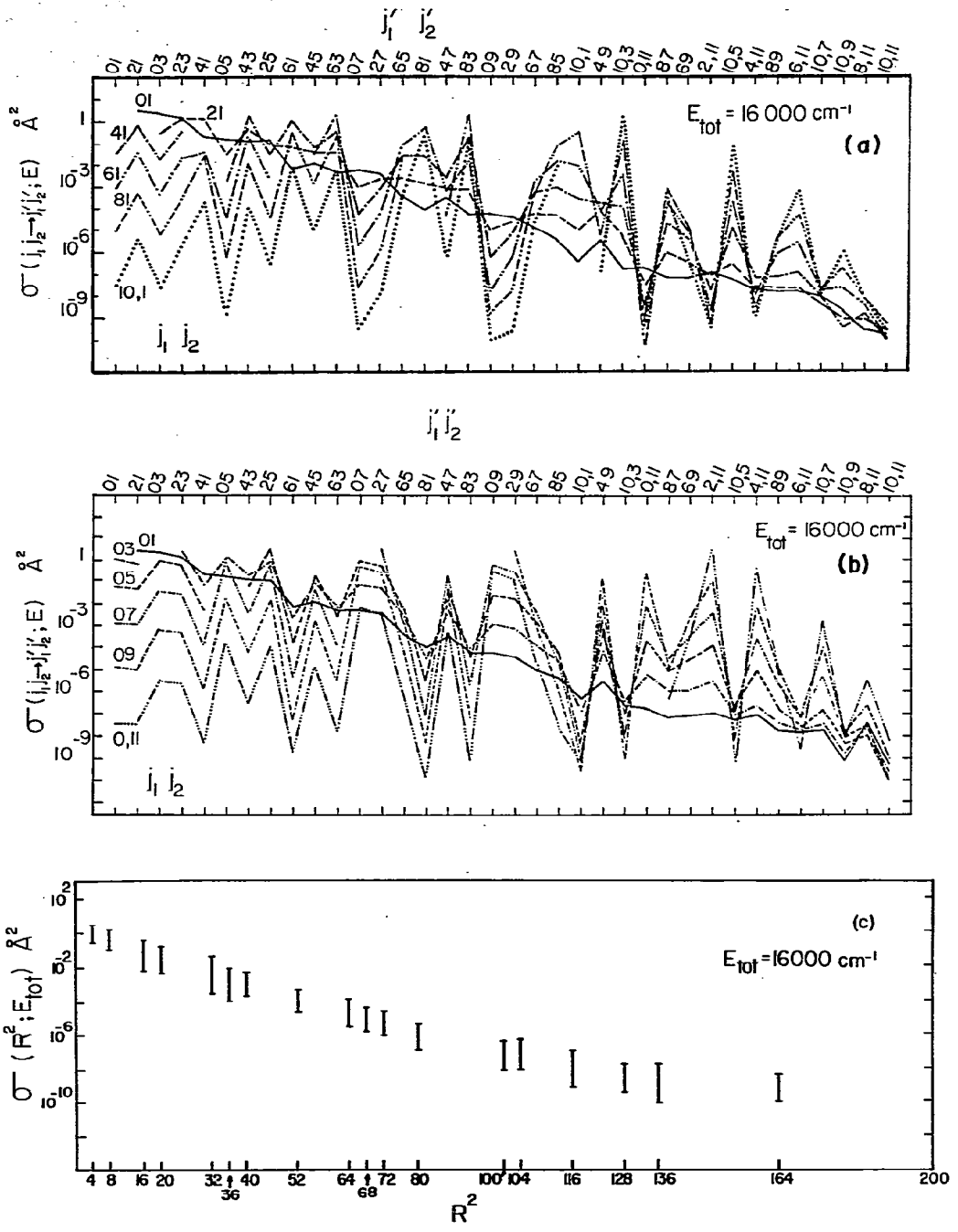

Fig. 3. (a) Cross section curves, $\sigma(j_1, 1 \to j_1' j_2'; E_{tot} = 16000\ cm^{-1}) j_1 = 0, 2, 4, ..., 10$. (b) Cross section curves, $\sigma(0 j_2 \to j_1' j_2'; E_{tot} = 16000\ cm^{-1}) j_2 = 1, 3, 5, ..., 11$. (c) Cross sections versus R^2 [defined in eq. (4)] at a fixed total energy of 16000 cm^{-1}.

ground rotational levels; hence every transition from this state is an excitation. If the final states are ordered energetically [cf. figs. 3a and 3b], the energy difference, $\Delta\mathcal{E} = \mathcal{E}_{j_1'j_2'} - \mathcal{E}_{01}$, increases monotonically, as does the R^2 value associated with each transition. The final states $j_1'j_2'$ can be divided into subsets, states of which have the same R^2 value for the transition $01 \rightarrow j_1'j_2'$, i.e.

$R^2 = 4 \quad j_1'j_2' = 03, 21$,

$R^2 = 8 \quad j_1'j_2' = 23$,

$R^2 = 16 \quad j_1'j_2' = 41, 05$,

$R^2 = 20 \quad j_1'j_2' = 25, 43$.

Within each subset the cross sections decrease as the energy transfer increases: $\sigma_{01\rightarrow 21} > \sigma_{01\rightarrow 03}$; $\sigma_{01\rightarrow 41} > \sigma_{01\rightarrow 05}$ etc., thus showing the *primary* dependence of the cross sections on coupling effects. Therefore, the distinctive appearance of $\sigma(01 \rightarrow j_1'j_2'; E)$ is fully consistent with the other curves when it is understood how these curves are correlated.

When cross sections at the same *kinetic* energy are correlated with R^2, the band structure of fig. 3c is retained (cf. fig. 4). The bands narrow at larger values of the fixed total energy which is to be expected, since the spread in the bands is due mainly to energetic effects that diminish in importance as the kinetic energy increases. It is quite apparent that the cross sections are well correlated with R^2. Since an entire collection of initial and final states is included in fig. 4 (o–o, p–p and o–p), this kind of correlation is helpful in estimating the magnitudes of all relevant cross sections.

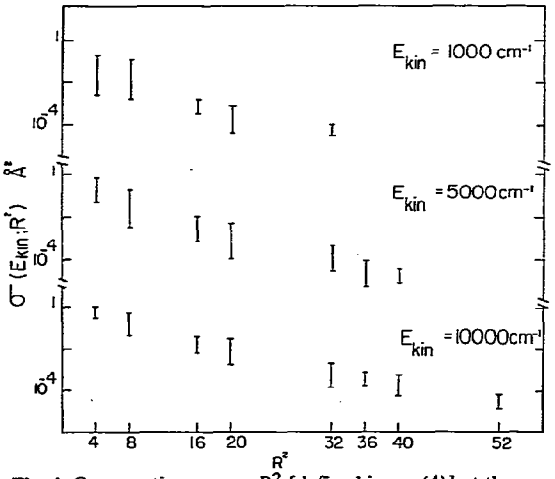

Fig. 4. Cross sections *versus* R^2 [defined in eq. (4)] at the same *initial* kinetic energy for three values of the kinetic energy.

3.2. The rotationally inelastic collision as a diffusion process

Inelastic collisions have been considered as a diffusion of probability between quantum states [12, 13]. In this treatment a master equation or Fokker–Planck equation is formulated to describe the time evolution of a collisional system. The effect of the collision is then to induce the diffusion of probability among the molecular levels. The H_2–H_2 system has not yet been studied in the stochastic formalism; however, the discussion below will show that these rotational processes are suggestive of diffusion-like behavior.

It is convenient to define a matrix of cross sections, $\boldsymbol{\Sigma}^E(j_1j_2)$, which is parametrically a function of j_1j_2. The elements of this matrix are given by

$$[\Sigma^E(j_1j_2)]_{j_1'j_2'} \equiv \sigma(j_1j_2 \rightarrow j_1'j_2'; E_{\mathrm{tot}} = E + \mathcal{E}_{j_1j_2}),$$

where the rows and columns are labeled j_1' and j_2', respectively. Considering oH$_2$–pH$_2$ collisions, we observe that j_1' has six possible values in this study, $j_1' = 0, 2, 4, \ldots, 10$, and j_2' also has six possible values, $j_2' = 1, 3, 5, \ldots, 11$. Hence the dimensionality of each $\boldsymbol{\Sigma}^E(j_1j_2)$ matrix is 6×6. At a given value of E there are also thirty-six possible initial states j_1j_2 for oH$_2$–pH$_2$ (i.e., thirty-six different $\boldsymbol{\Sigma}^E(j_1j_2)$ matrices).

We can now construct surfaces that are pictorial representations of these matrices by first setting the elastic cross sections $\sigma(j_1j_2 \rightarrow j_1j_2; E)$ arbitrarily equal to 100 Å^2. Cross sections less than 10^{-5} Å^2 are considered negligible and are therefore truncated to 10^{-6} Å^2 for convenience. This procedure is expedient for the comparison of the surfaces shown in fig. 5, as the highest and lowest points in *every* surface [figs. 5b–5f] are 100 Å^2 and 10^{-6} Å^2, respectively. Contours of constant cross section magnitude are drawn alongside each $\boldsymbol{\Sigma}^E(j_1j_2)$ surface to better illustrate the shape of the surfaces. These contours were obtained by linear interpolation along the rows and columns of the $\boldsymbol{\Sigma}^E(j_1j_2)$ matrices.

The diagrams in fig. 5 can be examined in two ways. First, the elements of the $\boldsymbol{\Sigma}^E(j_1j_2)$ matrices increase

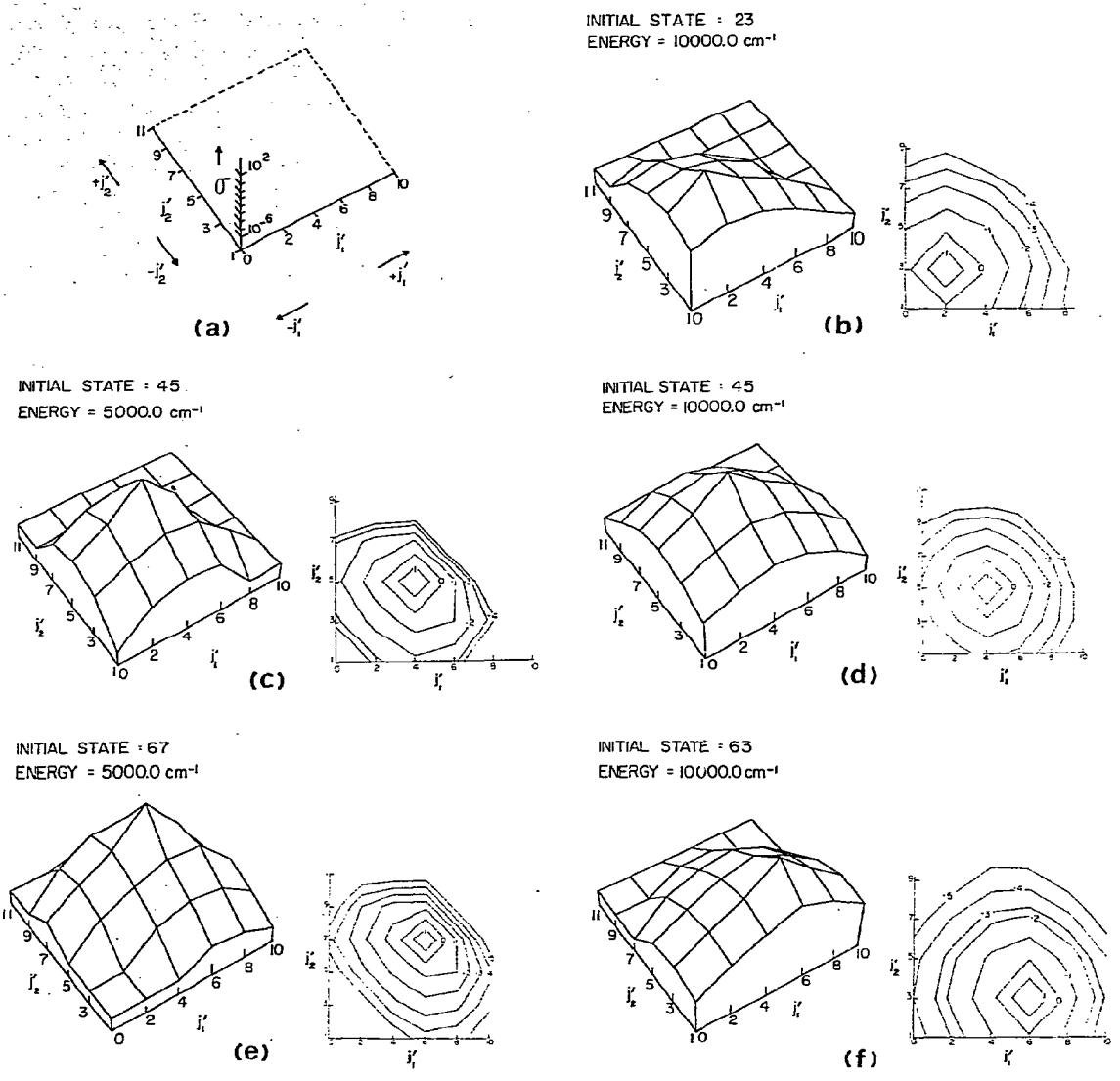

Fig. 5. (a) Scale used in (b)–(f). Directions of increasing and decreasing rotational quanta are denoted + and –, respectively. (b)–(f) Cross section surfaces $\Sigma^E(j_1 j_2)$ represented pictorially; $j_1 j_2$ is the initial state and E is the initial kinetic energy. The accompanying contours of equal cross sections are obtained by interpolation.

with increasing E. The surfaces are sharply peaked around the elastic cross section at low energies when not many final states are energetically accessible (cf. fig. 1). It is useful to compare figs. 5c and 5d which have the same initial state 45 but differ in the kinetic energy E. Fig. 5d has a broader peak, and this change is reflected in the corresponding contour plot by a spread (i.e., an increase in the separation) between the contour lines. Now define the $+j_1'$ and $+j_2'$ directions corresponding to increases in the para- and ortho-states, respectively (cf. fig. 5a)]. With this definition the $+j_1'$ and $+j_2'$ directions represent excitation while the $-j_1'$ and $-j_2'$ directions correspond to deexcitations. We see that lines of equal cross sections are not circular

about the initial state but are closer together in the $+j_1'+j_2'$ direction and further apart in the $-j_1'-j_2'$ direction. This structure is to be expected since the energy difference, $\Delta\mathscr{E}$, increases along the $+j_1'+j_2'$ direction. This leads to a rapid fall-off in the cross sections and thereby decreases the separation between the lines of equal cross section. Along the $-j_1'-j_2'$ direction, on the other hand, $\Delta\mathscr{E}$ increases less rapidly for the deexcitations and the consequent fall-off in the cross sections is more gradual. This then leads to larger separations between the contours.

Three different types of molecular states $j_1 j_2$ can be characterized as follows:

Corner state: j_1 and j_2 are ground states: 01,

Edge states: either j_1 or j_2 is a ground state,

Inner states: neither j_1 nor j_2 are ground states.

It is clear that corner, edge and inner states have, respectively, 2, 3 and 4 nearest neighbors (i.e., those involving $\Delta j = 2$). The strongest coupling is between immediate neighbors, and this results in an "edge effect" [14], producing a slight increase in cross sections for edge and corner states.

An important observation is that all the $\boldsymbol{\Sigma}^E(j_1 j_2)$ surfaces at a given energy are largely displacements of one another. The general shape of the surface is retained (compare figs. 5b and 5d or figs. 5c, 5e and 5f) with only a transferral of the peak to a new $j_1 j_2$ location in the grid. Energetic and coupling effects are responsible for the minor differences apparent in the contours.

The in-phase oscillatory nature of the cross sections in figs. 3a and 3b is consistent with the observation that the surfaces of figs. 5b–5f are approximate displacements of one another. It is therefore profitable to view the collisional process in terms of such surfaces, which is strongly suggestive of diffusion-like behavior in a nearly isotropic $j_1 j_2$ space. Similar behavior has been observed in model one-dimensional diffusion calculations [12]. It remains for further research to show that a stochastic approach can be applied to this system.

The above discussion was exclusively based on oH_2–pH_2 collisions. For identical molecule collisions, oH_2–oH_2 or pH_2–pH_2, the $\boldsymbol{\Sigma}^E(j_1 j_2)$ matrices are, in general, not easy to interpret since each matrix is actually a superposition of a direct and exchange matrix [see eq. (3)]. In the event that $j_1 = j_2$, however, the matrix becomes symmetric since the direct and exchange terms are equal. Examination of the surfaces $\boldsymbol{\Sigma}^E(55)$ and $\boldsymbol{\Sigma}^E(44)$ reveals that they are almost coincident in shape and magnitude with $\boldsymbol{\Sigma}^E(45)$ over the range 10^{-2} Å $\leqslant \sigma \leqslant 10^2$ Å and at $E = 10000$ cm^{-1}. Hence the cases of oH_2–oH_2 or pH_2–pH_2 collision processes are similar to the oH_2–pH_2 case, and in fact, this similarity is indicative of a redundancy in the information content of these surfaces. It should therefore be possible to reasonably estimate some of the o–p surfaces given the relevant corresponding o–o and p–p $\boldsymbol{\Sigma}^E$ surfaces.

3.3. Cross section behavior

The large basis sets needed in this calculation put comparable close coupled calculations well out of the question. A bench mark is, however, essential in judging the quality of the computed cross sections. Since rotational cross sections converge rather rapidly, limited basis CC and coupled states (CS) [6] calculations were performed at the same energies to obtain comparative cross sections for transitions between the lowest levels. While there have been many studies of the accuracy of the various approximate methods, the peculiarities of the system, the intermolecular potential and the energy range of the calculation make it difficult to arbitrarily extend the observations on one system to another. These limited exact calculations could, in addition, provide a means for scaling the extensive but approximate results.

Table 1 presents these tests at a few selected energies. The almost exact agreement between CC and CS cross sections is remarkable. Unfortunately, even with the CS effective hamiltonian method, calculations of the size reported in this paper would be prohibitively expensive. It must be pointed out that the peculiarity of *edge* and corner states leads to some misleading results. For example, at 12000 cm^{-1}, $\sigma^{CC}(01 \to 03) < \sigma^{EP}(01 \to 03)$ while $\sigma^{CC}(21 \to 23) > \sigma^{EP}(21 \to 23)$. This then leads to the ordering $\sigma^{EP}(21 \to 23) < \sigma^{EP}(01 \to 03)$ when in fact, the ordering is $\sigma^{CC}(21 \to 23) > \sigma^{CC}(01 \to 03)$. However, it should be understood that these fine differences are hardly significant on the scale of variations in figs. 2–5. Such differences will show up on close examination as in fig. 6. Studies that would be sensitive to these fine details should use appropriate caution. Figs. 6a, 6b and 6c depict the cross sections for three classes of transitions as a function of energy above threshold. In fig. 6a at a given

Table 1
Comparison of CC [a], CS [b] and EP [c] methods for pH_2-oH_2 cross sections [d]

$j_1j_2 \rightarrow j_1'j_2'$	4000 cm^{-1}			8000 cm^{-1}			12000 cm^{-1}		
	CC	CS	EP	CC	CS	EP	CC	CS	EP
01 → 01	45.1	44.9	46.0	41.3	41.2	42.8	38.8	38.7	40.0
21	1.42	1.47	0.96	2.11	2.20	1.84	2.40	2.50	2.45
03	0.59	0.62	0.88	0.97	1.01	1.63	1.12	1.15	2.07
23	0.14	0.13	0.09	0.48	0.47	0.44	0.82	0.85	0.97
41	0.022	0.021	0.009	0.10	0.11	0.06	0.22	0.22	0.16
05	0.004	0.0037	0.0044	0.034	0.035	0.047	0.077	0.077	0.122
21 → 21	46.1	46.2	46.4	42.4	42.3	42.6	40.0	39.9	40.2
03	0.054	0.065	0.077	0.10	0.12	0.13	0.15	0.17	0.22
23	0.64	0.63	0.51	1.27	1.30	1.11	1.67	1.73	1.50
41	0.36	0.34	0.29	0.94	0.94	0.85	1.76	1.36	1.30
05	0.0012	0.0010	0.0008	0.0066	0.0071	0.0054	0.014	0.017	0.013
03 → 03	40.0	45.7	46.1	41.7	41.0	42.2	39.3	39.0	39.7
23	1.34	1.40	1.04	2.27	2.38	2.07	2.77	2.92	2.73
41	0.0064	0.0081	0.0054	0.20	0.25	0.18	0.04	0.049	0.037
05	0.15	0.14	0.17	0.62	0.61	0.80	0.94	0.96	1.32
23 → 23	47.3	47.3	47.0	44.3	44.3	43.2	42.3	42.3	41.0
41	0.076	0.091	0.098	0.094	0.126	0.127	0.13	0.16	0.15
05	0.024	0.016	0.015	0.054	0.052	0.048	0.075	0.082	0.078
41 → 41	48.0	48.0	48.0	44.9	44.9	44.7	43.2	43.1	43.7
05	0.95(−4)	0.13(−3)	0.56(−4)	0.29(−3)	0.4(−3)	0.18(−3)	0.6(−3)	0.9(−3)	0.38(−3)

a) Close coupling. b) Coupled states. c) Effective potential.
d) The 0-CI interaction potential was used. The cross sections $\sigma(j_1j_2 \rightarrow j_1'j_2'; E_{\text{total}})$ are in units of A^2. All calculations included the six basis states, j_1j_2: 01, 21 03, 23 41, 05.

energy the ordering in the class $j_1 1 \rightarrow j_1 3$ is in terms of increasing j_1 save for the exception mentioned above. While the collision is in effect elastic for the para molecule, the fact that the "perturber" molecule possesses angular momentum does affect the processes [2, 15]. The contrasting family $0j_2 \rightarrow 2j_2$ in fig. 6b shows a similar ordering in terms of increasing j_2 at lower energies, while some alteration in this behavior occurs at higher energies where the curves level off. Fig. 6c shows the family of cross sections $0j_2 \rightarrow 0j_2 + 2$ along the edge $j_1 = 0$. Since the energy defect for each transition increases as j_2 increases, the ordering is according to decreasing j_2. There is also apparently a residual "corner" effect that enhances the 01 → 03 cross sections.

4. Conclusion

The general behavior of high-energy rotationally inelastic collisions in H_2-H_2 has been examined in this paper. The large number of possible processes gives rise to considerable complexity. Nevertheless, it is shown that the cross sectional behavior can be correlated with a parameter based on the change in angular momentum associated with each transition. The regular dependence of the magnitude of the cross sections on this parameter makes possible the estimation of cross sections for processes not considered here.

Cross sections from any given initial state at a fixed initial kinetic energy in oH_2-pH_2 collisions were analyzed in terms of a matrix. The three-dimensional representations of these matrices (viz. cross section surfaces) were seen to be largely similar regardless of the initial state and in spite of widely different energy gaps. As the dominant correlation was with the angular momentum parameter, the main factor in the

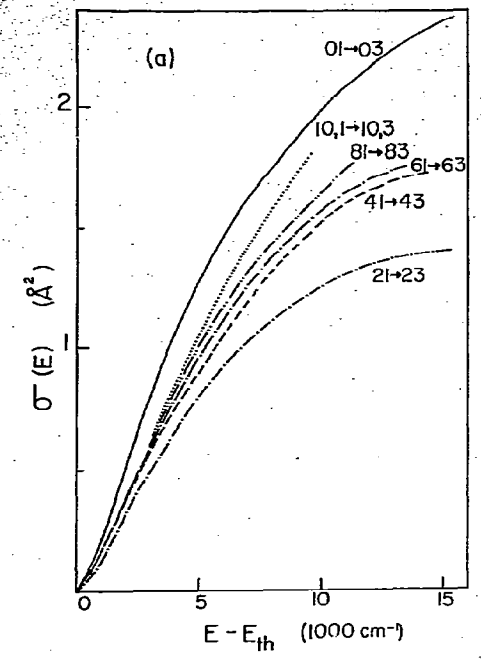

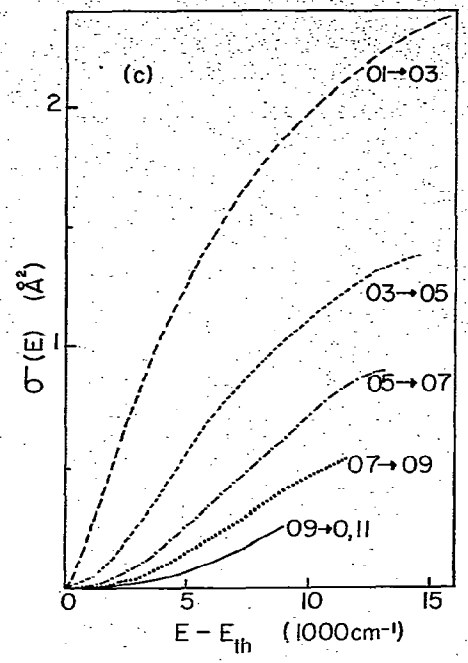

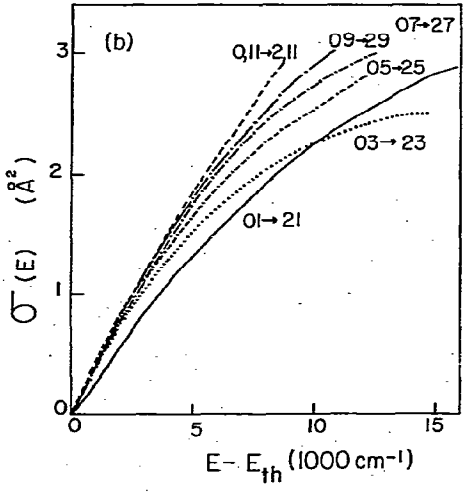

Fig. 6. Effective potential cross sections for various transitions in oH_2–pH_2 collisions versus the energy above threshold. (a) $j_1 1 \rightarrow j_1 3, j_1 = 0, 2, 4, ..., 10$; (b) $0j_2 \rightarrow 2j_2, j_2 = 1, 3, 5, ..., 11$; (c) $0j_2 \rightarrow 0j_2 + 2, j_2 = 1, 3, ..., 9$.

collisions is coupling rather than energetics. This would suggest that the sudden approximation [16] may also be valid in this system at such high energies.

The shape of the cross section surfaces indicates diffusion-like behavior in a nearly isotropic rotational space. This view of the collisional process can be treated in the stochastic approach, a method well suited to the handling of large numbers of molecular levels. It may well be possible to examine the influence of the vibrational levels in this system using this latter method.

References

[1] J.P. Toennies, Ann. Rev. Phys. Chem. 27 (1976) 225; D. Secrest, Ann. Rev. Phys. Chem. 24 (1973) 379; R. Gordon, W. Klemperer and J. Steinfeld, Ann. Rev. Phys. Chem. 19 (1968) 215.

[2] G. Zarur and H. Rabitz, J. Chem. Phys. 60 (1974) 2057.

[3] S. Green, J. Chem. Phys. 62 (1975) 2271.

[4] A.E. DePristo and M.H. Alexander, J. Chem. Phys. 66 (1977) 1334.

[5] R. Ramaswamy, H. Rabitz and S. Green, J. Chem. Phys. 66 (1977) 3021. In tables 1 and 2 and figs. 4 and 5 of this paper, the transitions $ij \rightarrow kl$ should in fact read in the reverse direction, (i.e., $ij \leftarrow kl$). In fig. 4b the energy variable should be $E_{\text{total}} - [\epsilon_{22} - \epsilon_{02}]$.

[6] H. Rabitz, in: Modern theoretical chemistry, Vol. 1A, ed. W.H. Miller (Plenum Press, New York, 1976).

[7] D.L. Merrifield and N. Ostlund, Intern. J. Quantum Chem; Symposium No. 11 (1977), to be published.

[8] N. Ostlund, private communication.
[9] G.A. Galiup, Mol. Phys. 33 (1977) 943.
[10] R. Ramaswamy and H. Rabitz, J. Chem. Phys. 66 (1977) 152.
[11] S. Green, R. Ramaswamy and H. Rabitz, Astrophys. J. Supplement (1977), to be published.
[12] S.D. Augustin and H. Rabitz, J. Chem. Phys. 64 (1976) 1223.
[13] G. Schatz, F. McLafferty and J. Ross, J. Chem. Phys. 66 (1977) 3609.
[14] S. Tarr, J. Sampson and H. Rabitz, J. Chem. Phys. 64 (1976) 5291.
[15] O. Crawford, Chem. Phys. Letters 6 (1972) 409.
[16] R.T Pack, J. Chem. Phys. 60 (1974) 633.